DEVELOPMENT AND OPTIMIZATION OF A HYBRID ROCKET ENGINE

M. Kobald, H. A. Moser, A. Bohr, S. Mielke,
HyEnD Stuttgart, Pfaffenwaldring 31, 70569 Stuttgart, Germany

Abstract

HyEnD (Hybrid Engine Development) Stuttgart, a student group of DGLR (German Aerospace Association) Stuttgart was founded in 2006 with the goal of building and developing a 2000 N hybrid rocket engine and the corresponding mobile test bench. Hybrid rocket engine means that fuel and oxidizer are provided in different aggregate states. The engine is based on solid paraffin as fuel and liquid nitrous oxide (N_2O) as oxidizer. This safe combination allows the use for educational purposes.

Paraffin as fuel is chosen due to its high regression rate. This rate is almost 3 to 4 times higher compared to conventional hybrid fuels. The decision for liquid nitrous oxide as oxidizer is made under consideration of its two main benefits: it is self-pressurizing which allows the use of a blow-down oxidizer supply system and it is neither toxic nor dangerous. Even the mixture of paraffin and nitrous oxide is estimated as inherently secure.

The first engine W2000 is developed for a desired design thrust of 2000 N at a chamber pressure of 20 bar for a burning time of 10 s. Two redundant main valves control the oxidizer supply system fed by multiple tanks. A Venturi tube measures the oxidizer mass flow and an additional sensor provides the pressure in the thrust chamber. The maximum mass flow is constrained by the injector geometry. This injector is especially developed and tested for the cylindrical fuel block to guarantee an optimal spray and swirling of the mixture. In combination with a pre- and post-combustion chamber high combustion efficiencies are achieved. The burning gases are expanded in a nozzle to ambient pressure. It is designed as a thrust optimized parabolic nozzle.

The engine is mounted on the mobile test bench by linear bearings and withstands thrusts up to 10 kN. The thrust is measured by a load cell. The control and measuring electronics are located under the mounting plate of the test bench and remote controlled via Ethernet. In conclusion this paper shows the development and optimization of a hybrid rocket engine by students and possible future developments.

1. INTRODUCTION

1.1. Hybrid rocket engines

The basic idea of hybrid rocket engines is to unite the simplicity and the storage behaviour of solid fuels with the controllability and reignition capability of liquid rocket engines. The disadvantages of those two extremes as toxicity, high safety risk or large material or control efforts are prevented. Furthermore straightforward control of mixture ratio by variation of the oxidizer mass flow and the immediate shut-down by closing the oxidizer's main valve is possible.

Their simplicity and high safety in handling makes them an excellent opportunity for academic and educational purposes at university for a student group. Projects like this offer a great possibility for students during their academic studies to apply all the theory they learnt and get real on-the-hands experience in developing, calculating, actually building and operating real hardware.

A wide field of knowledge from lectures at university like thermodynamics, space systems, chemical propulsion, aerodynamics, engineering mechanics, electronics and data processing, software design and project management has been applied during that project.

Historically hybrid rockets are first mentioned in 1929 by H. Oberth [1] who proposed a rocket composed of patent coal and liquid oxygen (LOX). In 1933 S. P. Korolev and M. K. Tikhonravov built the first hybrid rocket flying to an altitude of 400 m. A lot of work was performed in the 1960s at ONERA with the Lithergol experimental series (LEX) [2]. They built a controllable hybrid rocket with a hypergolic propellant combination based on red fuming nitric acid (RFNA) and an amine fuel. They conducted eight successful flights reaching altitudes of more than 100 km.

In the United States the United Technology Center (UTC) developed an upper stage hybrid engine using fluorine, lithium, lithium hydride and hydroxyl terminated polybutadiene (HTPB) as propellants. The most well known application of a hybrid rocket engine is the one flown on June 21, 2004: SpaceShipOne designed by ScaledComposites achieved the first privately funded human spaceflight.

1.2. Hybrid Engine Development Stuttgart

HyEnD (Hybrid Engine Development) Stuttgart, a student group of DGLR (German Aerospace Association) Stuttgart was founded in 2006 with the goal of building and developing a 2000 N hybrid rocket engine for a burning time of 10 s and the appropriate mobile test bench. The approach to reach these objectives is described in the following sections starting with the selection of the hybrid composition.

2. HYBRID COMPOSITION

There are two types of hybrid engines. One is the standard hybrid which is composed by a solid fuel block and liquid oxidizer. The second type is the so called inverse hybrid where the oxidizer is solid and fuel is added

in liquid state. This type is unusual due to the challenges of handling solid oxidizers and the resulting loss of safety and reliability. Since safety issues are of main interest the first decision is to define an appropriate combination of a solid fuel and a liquid oxidizer. Some hybrid propellant combinations like LOX/HTPB offer equal performance to liquid bipropellant systems as LOX/Kerosene [3].

2.1. Choice of fuel

Commonly used fuels are polymeres like HTPB, polyethylene (PE), polyvinyl chloride (PVC), polymethylmethacrylate (PMMA), polypropylene (PP) and polybutadiene acrylonitrile (PBAN). Most of these fuels can be easily cast into the desired shape, are mechanically stable and non-toxic. Here a possible application of hybrid engines can be investigated in the future: The throw away of the International Space Station (ISS) which is currently expanded i.e. in the Automated Transfer Vehicle ATV is assumed to be mainly composed by plastics. These plastics could act as fuel for hybrid engines which recycle the plastics by accelerating the station. This idea is kept in mind and requires more investigations mainly in the field of melting and casting the plastics into a fuel grain and the general handling.

The drawback is their low regression rate. The mass flow from the solid fuel into the combustion zone is defined by the heat of vaporization of the fuel and the heat transfer. It is estimated as shown in equation (1):

$$\dot{m}_f = \rho_f \, A_s \, \dot{r} \tag{1}$$

The fuel mass flow is proportional to fuel´s density ρ_f, its surface A_S and the regression rate $\dot{r}$. To achieve appropriate mass flows and high overall thrust with these fuels a high surface area is needed. Therefore long fuel grains with multiple ports are necessary which results in a low volumetric efficiency [4].

In the last years a new kind of fuel has been researched at Stanford University, so called liquefying hybrids [5]. These fuels are paraffin-based hydrocarbons and show a regression rate 3 to 4 times higher than in conventional fuels. These high values are achieved by entrainment mass transfer. Normal polymeric fuels need to be fully vaporized before being burned. Paraffin-based hydrocarbons form a melt layer on the surface on the fuel. From that layer liquid droplets are entrained by liquid layer instabilities. Those are caused by the high velocity gas flow in the combustion chamber [6]. Therefore much more fuel can be transported into the flame zone before being totally vaporized. Scale-up tests have also been done confirming that the theory is applicable even for large engines [7].

Due to the listed advantages of paraffin-based fuels these are used for the first investigations and developments. The according oxidizer is selected in the following section.

2.2. Choice of oxidizer

Most of the oxidizers used in space propulsion like nitrogen tetroxide (N_2O_4) or hydrogen peroxide (H_2O_2) provide a good performance and are depending on the fuel hypergolic however they are also difficult to handle and very toxic. Possible nontoxic oxidizers are air, pure oxygen or nitrous oxide.

Pressurized gaseous oxygen could be used but the density is too low for the desired thrust. LOX would be the oxidizer with the highest performance, but also requires high precautions for a safe handling. Due to these facts nitrous oxide (N_2O) is selected. At 25°C the vapour pressure is at 55 bar hence self-pressurization to feed the oxidizer system with liquid nitrous oxide is possible. It is well storable, easy and with a moderate price to purchase, and has a relative high density.

The self-pressurization provides the advantage of a simple oxidizer feed system with no additional pressuring gas or even pumps. The critical point of N_2O is at 36 °C which results in large density variations over the temperature range in which it is being used. Due to the low critical point all calculations involving ideal gas assumptions lead to inaccurate results in predicting the tank pressure [8], [9]. Therefore real gas properties are assumed and extra simulations are developed.

The performance and thrust in a self-pressurizing hybrid rocket depends directly on the oxidizer mass flow. It is calculated from the pressure difference between tank pressure and chamber pressure. For the accurate prediction and to model the performance an ambitious two-phase model for the tank pressure considering real gas effects has been developed.

2.3. Preliminary design calculations

The initial design requirement for the engine is a thrust level of 2000 N. To determine the required mass flow the specific impulse (I_{sp}) has to be identified. The relation between thrust F, for a nozzle expanding to ambient pressure, and I_{sp} is

$$F = \dot{m} \, c_e \quad \text{and} \tag{2}$$

$$\mathrm{I_{sp}} = \frac{c_e}{g}. \tag{3}$$

Total mass flow $\dot{m}$ is defined as the sum of oxidizer mass flow $\dot{m}_{ox}$ and fuel mass flow $\dot{m}_f$. For test data performance evaluation, the actual characteristic velocity c^*_{act} [7] can be calculated with

$$c^*_{act} = \frac{\int_{t=0}^{t=t_b} p_c(t) \cdot dt}{(m_f + m_{ox}) \, c_{dn} \, A_t} \tag{4}$$

and further compared with the theoretical c^*_{theo} to get an efficiency of combustion η_c

$$\eta_c = \frac{c^*_{act}}{c^*_{theo}}, \tag{5}$$

where c_{dn} is the discharge coefficient of the nozzle, A_t the area of the nozzle throat, and p_c the chamber pressure integrated over time t. The c^*_{act} correlates with the I_{sp} by

$$\mathrm{I_{sp}} = \frac{c^*_{act} \, c_F}{g} \tag{6}$$

Assuming a constant coefficient of thrust c_F the I_{sp}. can be derived from equation (6). Several programs exist that perform the extensive thermochemical calculations during a combustion process. We chose the NASA (National Aeronautics and Space Administration) program CEA (Chemical Equilibrium with Applications) to calculate values of I_{sp} and c* depending on the oxidizer-to-fuel ratio O/F. For the first tests data was calculated for a fuel grain consisting only of paraffin. A significant increase in performance and I_{sp} can be observed with the addition of aluminium to the fuel. While the I_{sp} is increasing the O/F is decreasing thus reducing the mass of nitrous oxide needed. Adding aluminium increases the combustion temperature which results in a higher heat flux to the fuel therefore a higher regression rate. The oxidizer mass flow is defined as

$$\dot{m}_{ox} = c_d \, A_{inj} \sqrt{2 \rho_L \, (p_{tg} - p_c)} \, . \tag{7}$$

The pressure difference (p_{tg}–p_c) between tank and combustion chamber and the density of the liquid oxidizer ρ_L influence the oxidizer mass flow less than the injector surface area A_{inj} and the discharge coefficient c_d of the injector.

After having determined the oxidizer mass flow, the fuel mass flow can be estimated with equation (1) and the regression rate

$$\dot{r} = a \, p_c^{\alpha} \, G_{ox}^{n} \, L^{m} \tag{8}$$

with the fuel dependent constant a, the regression rate exponent n, the chamber pressure p_c and the pressure exponent α. Furthermore the length of the fuel grain L with the length exponent m and the oxidizer mass flux

$$G_{ox} = \frac{\dot{m}_{ox}}{A_p} \tag{9}$$

are included. The oxidizer mass flux is defined by the oxidizer mass flow and the cross-sectional area of the fuel port A_P through which the oxidizer is flowing.

The regression rate of the paraffin-based fuels shows no pressure dependency hence the term containing the chamber pressure can be neglected [7]. The influence of the length of the fuel grain is also negligible therefore the equation for the regression rate can be simplified to

$$\dot{r} = a \, G_{ox}^{n} \, . \tag{10}$$

The distribution of thrust and regression rate during a test is calculated with a Matlab-Simulink model. The length of the fuel grain is varied until the average O/F over burn time reaches the optimum O/F. As an additional input the oxidizer mass flow is required. Due to the real gas behaviour of nitrous oxide as described above another extensive model is integrated. It calculates the distribution of mass flow, temperature, pressure and other relevant values in the oxidizer tank during the blow-down operation.

The advantages of paraffin as a fuel can be seen when calculating the sizes of a hybrid rocket engine with the same thrust of 2000 N and for example PE [10] as fuel. With paraffin a short cylindrical grain with only one port is sufficient, which can be burnt almost totally thus enabling a high volumetric efficiency. With PE a much longer grain with 5 to 6 ports would be needed to achieve the same result.

3. FACILITIES

The main components of the engine and the mobile test bench are described in the following subsections.

3.1. The engine W2000

W2000 as indicated in Figure 1 is mainly designed to account for student use. To reach the main objective of studying the general behavior of hybrid rocket engines a robust design is chosen. Consequently the ease of manufacturing and margins for additional improvements are considered. The use of standardized parts as the flanges for the nozzle and the injector plate are an example for that approach.

Figure 1: Engine W2000 at full operation

3.1.1. Oxidizer supply system

The oxidizer supply system is designed with the constraints of the oxidizer mass flow into the combustion chamber. Constant pressure loss is given by the length of the pipelines complemented by losses of devices in the line as valves, fittings for sensors or connections. With a Venturi pressure measuring device the mass flow in the oxidizer supply pipeline is measured. Two electrically actuated solenoid valves in series are used for redundancy and give the possibility for an immediate shutdown.

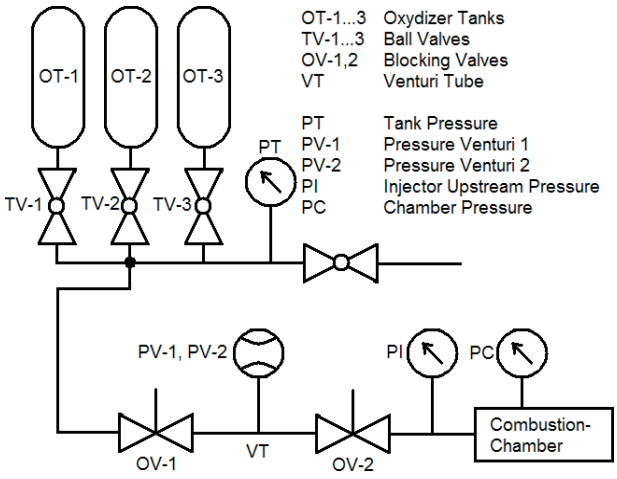

Figure 2: Oxidizer feed system

Figure 2 shows the block diagram of the oxidizer feed system. The nitrous oxide is stored in three high pressure tanks OT-1 to OT-3. Each tank is connected to the feed line via a mechanically actuated ball valve TV-1 to TV-3. Depending on the desired mass flow and burn time a test can be conducted with a single tank, but also with two or three in parallel. The tank outlet pressure PT is measured at the connection of the three tanks directly after the ball valves TV-1 to TV-3. A separate ball valve is used for filling of the tanks where PT allows pressure control.

A short flexible tube connects the tanks with the first upstream solenoid valve OV-1. Between the first OV-1 and the second solenoid valve OV-2 a Venturi tube VT is located. Two pressure sensors PV-1 and PV-2 measure the pressure difference along the Venturi tube. Complemented with the density of the liquid nitrous oxide the mass flow during a test is calculated with the developed tank pressure simulation.

After the second solenoid valve OV-2 upstream of the combustion chamber another pressure sensor is located PI. The combination of the different pressure sensors allows the calculation of the relevant pressure losses in the system. The pressure sensor system is complemented by the camber pressure sensor PC.

3.1.2. Injection system

Ensuring a stable combustion it is essential that the paraffin and nitrous oxide are mixed homogenously. Therefore the liquid oxidizer has to be atomized sufficiently. Besides the definition of maximum mass flow this atomization of the oxidizer is the main task of the injector head.

Atomization can be performed with thermal or mechanical treatment of the liquid. The mechanical treatment is atomizing by shear forces. Classical injector geometries are the swirl injectors and the impingement injectors. In a swirl injector the fluid flow is rotated and swirled. In impingement or impinging jet injectors a defined number of fluid jets are colliding with each other. Swirling ruptures the fluid into droplets of varying size.

Figure 3: Shadowgraph image of impingement-dome injector spray with water

According to the requirement of simple and robust design an optimum injector type has to be selected. A double impingement injector is excluded due to its formation of an elliptical flow pattern. This pattern is undesirable for a cylindrical wax grain. A triplet impingement injector results in a more advantageously spray shape but the manufacturing effort due to the high precision of the boreholes counts against this solution. The simplest injector is the showerhead which has a dedicated number of boreholes orthogonal to the injector surface. To get higher shear forces a modified showerhead is invented. In a simple showerhead the individual streams do not interact with each other. Here radii of the boreholes and length are the parameters where the vapour can be optimized in a dedicated range.

The introduced impingement-dome injector combines rapid mixing and atomization of the flow with simple manufacturing. The oxidizer stream is widened up with distance to injector exit surface into the thrust chamber. Figure 3 gives an impression of the spray shape. The characteristics of the injector are identified during tests with water performed at the M11 test facility of DLR (Deutsches Zentrum für Luft- und Raumfahrt) in Lampoldshausen. Figure 4 shows the control and data acquisition panel for the performed pressure and mass flow measurements. Here the different spray forms are qualitatively observed and also the characteristics like the

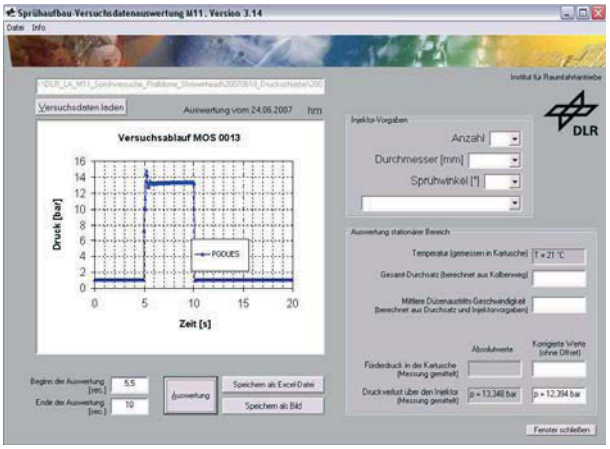

Figure 4: Snapshot of control and data acquisition panel of M11 test facility at DLR LA

pressure loss Δp over the injector head and the maximum oxidizer mass flow are determined.

For the dimensioning of the injector head it is assumed that the nitrous oxide is in liquid phase at the injector head inlet. The design mass flow of 1 kg/s is required for the desired performance. Therewith the area of the injector is calculated. A minimum pressure drop over the injector is defined to decouple the oxidizer feed lines from pressure oscillations in the thrust chamber. A value of 10 to 12 bar was desired in the initial design. We choose to manufacture two different injectors. On the one hand a simple showerhead injector has been realized with 3 concentric holes of 4 mm. Each hole has a length to diameter ratio L/D of 5. On the other hand a more advanced type was manufactured, the aforementioned impingement-dome injector. The geometry of the holes stays the same, yet at the end of the injector a cone is attached, which shall lead to rapid and homogenous atomization of the oxidizer. Besides the tests with water at

DLR, the performance of both injectors is also compared during the hot fire tests.

The complete injection system consists of the injector plate which is an adapted blind flange and a welded pipe connection for the different injector heads.

3.1.3. Combustion chamber

The combustion chamber is one of the central parts of the whole engine. It has to withstand stresses from the high chamber pressure during combustion. Even more significant are thermal stresses from combustion temperatures of approximately 3000 °C. These temperatures would require an active cooling concept of the thrust chamber for a small wall thickness. Therefore stainless steel 1.4541 with increased wall thickness is selected. This enables a passive cooling of the thrust chamber due to the high specific heat capacity of the steel. Another advantage is the additional safety margin.

The incoming oxidizer requires dedicated time to be atomized. Therefore a pre-combustion chamber is utilized.

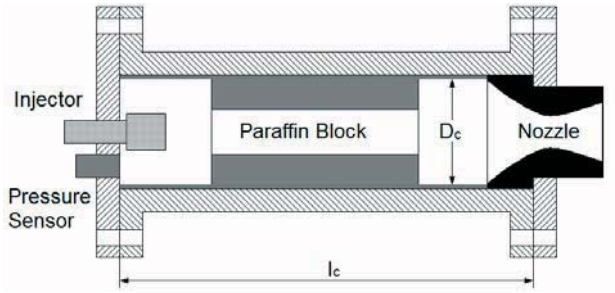

Figure 5: The schematic engine

It can be identified left from the paraffin grain in Figure 5. Typically hybrid engines only burn with a small diffusion flame in the boundary layer with a distance from the fuel surface of about 10% to 20% of the local boundary layer thickness [1]. Due to that small flame not all of the oxidizer and fuel can immediately react. To correct this incomplete reaction a post-combustion chamber (right from the paraffin grain in Figure 5) provides the residual time for the mixture hence the combustion efficiency improves. For the first version of the engine the pre-combustion chamber has a length of 30% of the fuel block length and the post-combustion chamber has a length of 30% to 50%. Combining casings of different length for the fuel and the pre- and post-combustion chamber, the location of the fuel grain in flow direction can be modified.

3.1.4. Nozzle

From overall power performance of an engine 80% are provided by the thrust chamber and 20% by the nozzle. This fact highlights the importance of the nozzle design. Due to the diverging profile of the nozzle, the subsonic flow from the thrust chamber is accelerated in the converging part and reaches sonic velocity in the throat. For further acceleration of the flow thus to get supersonic velocity the diverging contour is necessary. The shape of diverging and converging defines the type of nozzle.

There are three most widely used types or forms of nozzles:

- The simplest contour is the conical nozzle, also called Laval-nozzle. It consists of a converging-diverging contour, with constant gradient. These nozzles are easy to manufacture, but are not used very often because of their low efficiency.
- Ideal nozzles create a uniform, parallel flow at the exit to achieve a high thrust. The ideal contour is calculated with a method of characteristics. Because of the low gradient of the contour at the end, the nozzle can be shortened to save weight, called a TIC - Truncated Ideal Contour.
- At today's rocket engines (Vulcain II, Space Shuttle Main Engine) so called Thrust Optimized Contours (TOC) are used. These contours are calculated with a method of characteristics and a variation calculation, to get the maximum thrust. The calculated contour can be described with a parabola, a so called parabolic nozzle.

Figure 6: TOP nozzle (graphite)

For HyEnD a thrust optimized parabolic (TOP) nozzle is calculated. The advantage of that design in comparison with a Laval-nozzle is a higher efficiency and 80% of the Laval nozzle´s length, therefore less weight. The heat flow in the nozzle and therefore the temperature reaches a maximum in the throat. So the first nozzle is machined of graphite due to its very high sublimation temperature of 3973 K. That temperature lies well above the temperature of the combustion gases in the throat which is calculated to be 2800 K. So no sublimation of the graphite nozzle occurred during the tests. The nozzle was used during the first nine tests without any measurable erosion of graphite in the nozzle. After test 9 a crack has been observed in the nozzle. A possible reason is an eventually too high initial tension of the flange connected to the nozzle and combustion chamber.

Figure 7: Laval nozzle (steel)

Therefore a new nozzle is designed of stainless steel. The contour is a Laval design hence differences in the designs can be investigated. Both nozzles shown in Figure 6 respectively Figure 7 provide the same area ratio and are adapted to ambient conditions at ground, expanding the supersonic exhaust flow to 1 bar with a mach number of 2.5.

3.2. The mobile test bench

The mobile test bench shown in Figure 8 is designed to host engines up to 10000 N. It is made of standard steel profiles welded to resist the forces during a test. On top of the test bench an aluminium plate is mounted. The selected engine is attached to it with linear bearings. Those bearings are aligned in thrust direction that the engine's thrust can be measured by a load cell.

Both solenoid valves and the Venturi tube are also mounted on top of the test bench. They are also mobile in thrust direction. The electronics, the control laptop and power supply are safely located under the top plate.

Figure 8: Mobile test bench with oxidizer supply system and engine

The high pressure tanks are mounted directly behind the test bench on a concrete structure and are connected via a flexible tube. Additionally the test bench is anchored to the ground with M18 screws. Four wheels attached on the bottom frame of the testbench enable the mobility of the entire test bench.

3.3. Instrumentation and measurements

Figure 9: Under expansion and mach diamonds shortly after ignition

For data acquisition a Labjack measuring device is utilized. It provides eight analogous measuring inputs with a sampling rate of 10Hz. Two outputs are used to control the solenoid valves. The Labjack device converts the voltage signals from the sensors into a digital format. This data is recorded directly on the laptop mounted under the mobile test bench.

Especially developed software controls the predefined test sequence, records the data and closes the valves after the desired test time. Every pressure value is checked at instant and both valves can be closed automatically hence stop the test if any value exceeds the threshold. The laptop is remote controlled via an Ethernet network connection from a second laptop in a safe distance. In case of software or connection anomalies during a test, the engine can be shut off immediately by the test supervisor with an emergency shutdown switch.

In order to obtain a preferably full characterization of the engines operation a set of different sensors is attached to the system

- The thrust F of the engine is measured directly using a load cell with a measuring range up to 5000 N. This device can be replaced according to the desired load range.
- The oxidizer mass flow $\dot{m}_{ox}$ is measured indirectly by a Venturi tube.
- The chamber pressure p_c is measured directly by a pressure sensor.
- The pressure course along the pipelines is measured directly using a set of pressure sensors distributed throughout the oxidizer supply system (see Figure 2).

In addition to these real time measured values another set of values can be obtained

- The integral solid fuel mass consumption
  (11) $m_f = m_{f,2} - m_{f,1}$
  is determined by weighing the paraffin grain before and after operation.
- The integral oxidizer mass consumption
  (12) $m_{ox} = m_{Ox,2} - m_{Ox,1}$
  is determined by weighing the oxidizer tank before and after operation.

4. PERFORMANCE TESTS

In order to determine the correct operating point of the engine several performance tests as exemplary shown in Figure 9 are conducted. Further influencing parameters as

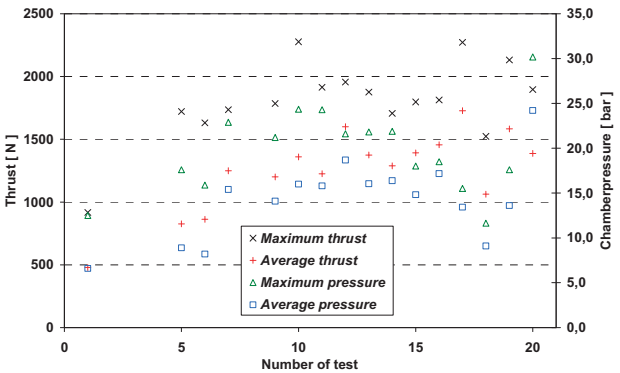

Figure 10: Test overview

the ideal O/F are varied and studied. Major criteria are the combustion chamber pressure and the characteristic of thrust during burning time. One parameter, the mass flow is also described in the following subsections.

The oxidizer supply system is the first major component to be optimized for the initial test runs. Especially the pressure losses throughout the systems components such

as injector, valves and pipelines are of particular interest. Therefore a set of pressure sensors is distributed throughout the oxidizer supply system in order to obtain a pressure course. For a better comparison the average thrust of each test is calculated with

$$\overline{F} = \frac{1}{t_b} \cdot \int_{t=0}^{t=t_b} F(t) \cdot dt \,. \qquad (13)$$

The integral mass consumption is also calculated and measured for each test with

$$m_f = m_{f,t=0} - m_{f,t=t_e} = \int_{t=0}^{t=t_e} \rho_f \cdot A_s(t) \cdot \dot{r}\,(t) \cdot dt \,. \qquad (14)$$

An exemplary value of burned fuel m_f is 0.287 kg for a burning time of 2.1 seconds during test 17.

20 performance tests were conducted until now. Here the behaviour of thrust and chamber pressure during operation was of particular interest. All test values are shown in the test overview in Figure 10 Not all boundary conditions, especially temperature and tank pressure, are constant in this overview. Maximum and average thrust

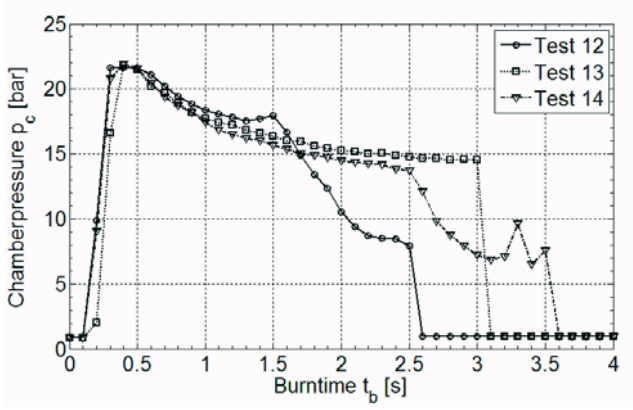

Figure 11: Chamber pressure over burning time

respectively chamber pressure are indicated. It shows the qualitative improvements of the performance tests in the tendency towards design thrust. Test 2 to 4 failed due to problems with blocked valves in the oxidizer supply. Test 8 was a successful run, with similar conditions in terms of fuel and tank pressure as in test 7 which was on the same day. No data of test 8 is available due to a malfunction in the electronic data acquisition during the test.

Consequently, since test 5 we increased the diameter of the oxidizer supply and replaced the first valves with coaxial valves, especially designed for high mass flows and low pressure losses. During test 5 and 6 thrust and pressure is already higher but rapidly decreasing because the gas bottle restricted the mass flow. So we chose lightweight high pressure carbon fibre reinforced plastic (CFRP) tanks with a greater exit diameter. Since then the oxidizer mass flow is high enough and the influence of the fuel grain length to the overall thrust could be observed.

For test 8 and 9 the fuel grain provides L/D of 10, which was expected from the initial design. But the total consumption of oxidizer and fuel indicated an average O/F of approximately 2 instead of 6-8 as expected. So for test 10 and 11 we reduced the L/D to 5.This resulted in an average O/F of about 4 and also a higher average thrust.

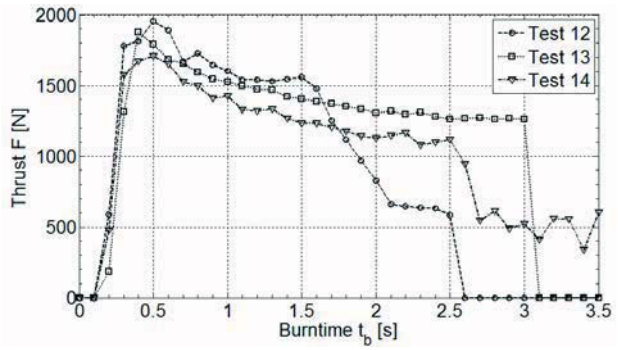

Figure 12: Thrust over burning time

Maximum thrust of test 10 was higher due to a higher initial tank pressure than in test 11. For test 12 to 16 we reduced the L/D in the range of 2.3 to 3 and thereby reaching an average O/F of 6. With this O/F of 6 being near at the optimum O/F of approximately 7-8 average thrust also slightly increased.

Exemplary the chamber pressure of three comparable test runs is shown in Figure 11. The thrust behaviour during burning time of these tests is shown in Figure 12 where the boundary conditions as fuel composition and fuel length are constant for the three runs. For test 12 and 13 the initial tank pressure was equal, while the tank pressure of test 14 was significantly lower due to a longer time outside in the cold. The burning time varies from 2.5 s for test 12 up to 3.5 s for test 14 in steps of 0.5 s.

Some of the main challenges for proper engine operation can be seen in these figures

- Thrust and chamber pressure of test 12 are equal with those of test 13 until 1.5 s. At this point the entire liquid phase of the oxidizer is consumed resulting in a huge drop of both values due to the significantly lower oxidizer mass flow.
- Thrust during test 14 is significantly lower than the one measured during the other two performance tests. The reason is the lower initial tank pressure during test 14, which results in a lower chamber pressure and therefore a lower overall thrust.
- During long duration performance tests a volatile burning behaviour corresponding with fluctuations of thrust and chamber pressure can be observed. This behaviour can partially be explained with a breaking apart of the paraffin fuel grain, as it can be seen in Figure 12 after 2.5 seconds after ignition of test 14.

After all optimizations to increase oxidizer mass flow and to find the proper length of the fuel grain we did not yet reach an average thrust of 2000 N. The combustion efficiency is expected to be lower than previously assumed in the design calculations. So for the last two tests 17 and 18 we increased the injector area. As it can be seen in Figure 10, the average thrust reaches the highest value of all tests in test 17, with 1728 N and a maximum value of 2272 N. Due to the higher mass flow in that test, the chamber pressure is lower than in the

previous tests.

Test 18 was done with comparable setup one hour after test 17. Fuel grain composition and length were the same, and initial tank pressure was 49 bar for test 17 and 47 bar for test 18. For test 1 to 17 we used our specially designed impingement-dome injector. In test 18 we replaced it with a normal showerhead, with the same effective area. Although the boundary conditions were the same, average thrust was only 1062 N with a maximum of 1523 N. Even tough the mass flow for test 18 was 15% higher than in test 17 thrust performance was very poor, indicating a very low combustion efficiency induced by the showerhead injector. This highlights clearly the importance of the developed injector and its spray efficiency. Due to the reduced L/D of the fuel grain during the tests we decided to build a second thrust chamber with a smaller length and mass, and the possibility to enhance the chamber pressure. In test 19 a short test was done and the newly designed thrust chamber worked as expected so we reduced the nozzle throat area for the next tests. With that new design we reached a maximum chamber pressure of 30 bar during test 20 and an average value of 24 bar.

Additionally to photos as Figure 9 video-data was recorded for each test, including normal perspectives and close-up views from the nozzle exhaust.

With these close-up views over- and under expansion during the transient start-up and shut-down phase of the engine operation are studied. First investigations show appropriate compliance with the recorded in-situ chamber pressure data.

5. CHALLENGES AND OPTIMIZATIONS

During the first tests the oxidizer supply system emerged as one neuralgic point. The initial design calculations of the combustion chamber, nozzle and injector were pretty accurate. The assumptions made for the pressure losses in the oxidizer feed system were too optimistic.

Nitrous oxide is used at its saturation pressure, so with each pressure drop in the feed system more nitrous oxide evaporates from the liquid to the gas phase. This evaporation gain lowers the pressure and the mass flow is also reduced due to the two-phase flow. One solution is to perform cold-flow tests where the pressure losses of the valves, feed line, Venturi tube and injector are measured. With these measurements new discharge coefficients are calculated. In comparison with previous cold-flow tests with water, the discharge coefficients are smaller.

Figure 13: Frozen water on the valve with attached Venturi tube

First the liquid nitrous oxide was supplied directly from a commonly available gas bottle and some standard valves and piping. During these tests the pressure losses were so high that almost only gaseous nitrous oxide arrived in the thrust chamber resulting in a very low chamber pressure and thrust. The huge pressure and temperature drops in the feed system are visible on the outside of the valves and tube where moisture from the air was frozen shown in Figure 13.

To reduce the pressure losses in the feed system the oxidizer flow velocity is reduced with new tubing of larger cross-sectional area. The valves are also replaced. With this improved equipment a significant increase in maximum thrust and also chamber pressure can be observed. Although the initial values of thrust and pressure are significantly larger than during the previous tests, thrust and pressure rapidly decreases after ignition (see Figure 11 and Figure 12). The reason for that behaviour was the last part restraining the mass flow instead of the injector: the exit of the gas bottle with only 4 mm diameter. Therefore the last optimization in the oxidizer supply system was to use tanks with a larger exit cross-sectional area. Lightweight high pressure CFRP tanks with a volume of 9 litres are the current equipment. To be prepared for future engine versions three of these tanks are parallel connected. On the one hand this enables longer burning times and on the other hand to increase the mass flow for higher thrust levels.

With these tanks a constant high mass flow, desired thrust level and chamber pressure are achieved as indicated in Figure 11 and Figure 12. The slow decrease of thrust and pressure in the figures reasons first to the decreasing regression rate over time. Second reason is the also decreasing pressure characteristic of the liquid nitrous oxide in the tanks due to evaporation.

In the current oxidizer feed system the largest pressure drop is currently in the injector. Since this is foreseen in the injector design the chamber pressure during the first tests is limited to approximately 20 bar. This assures that too high chamber pressures do not influence the mechanical stability of the fuel grain. After our last test with we are confident to reach average chamber pressure of more than 30 bar, which would also increase our I_{SP}.

6. CONCLUSION AND OUTLOOK

Conclusion

The initial objectives set are ambitious for a student project as presented in this document. The developed engine provides approximately 2000 N thrust proven in several tests. The initially desired burning time can be achieved by a thrust chamber with a greater diameter, which will be also the next step in improvement. To reach these goals optimizations as an improved oxidizer supply system or changes in the fuel composition and dimensions were necessary. The basic investigations of the oxidizer spray behaviour and the shape led to the development of new injector geometry for improved oxidizer vaporisation. This improvement was initially verified with further injector geometry for comparison. The adaptations can be performed due to the data acquired with the control and data acquisition system of the mobile test bench. This system and the according simulations are especially developed for the testing of hybrid rocket engines based on paraffin and self-pressurizing nitrous oxide. The oxidizer mass flow is also measured within the test bench equipped with thrust and pressure sensors and a Venturi tube.

Generally the successful development, testing and optimization of a hybrid rocket engine in a student group showed the potential to motivate students for practical applications of the theory especially in the Space propulsion sector.

Outlook

There are several directions and plans to be realized in the near future. One goal is to optimize the weight of the current engine W2000 and build a system including oxidizer feed system and tank that can be flown on a small scale sounding rocket. Preliminary design calculations for the rocket have been done. Furthermore the addition of high energetic particles will be proofed. A performance increase in I_{sp} can be gained by the addition of metal powders to the paraffin fuel, like aluminium [11].

A large influence from the injector on the combustion efficiency and therefore on the performance of the engine has been observed during our tests. So the study of the injector design and performance will also be one of the main aspects in the further development.

Another direction of further investigations is to optimize the motor for the use as kick-engine for small satellites. There the issue of re-ignition will be one major task to be observed. Furthermore the idea of the recycling engine for innovative synergisms onboard the ISS will be investigated in more detail, i.e. in studying the melting handling of PE and its possible automation.

7. ACKNOWLEDGEMENTS

The authors would like to thank all the persons, institutes and companies who supported the presented work in several manners especially the Klaus Tschira Stiftung GmbH for their fundamental sponsorship. A complete list of our supporters is presented under www.hybrid-engine-development.de.

8. REFERENCES

[1] R. Schmucker, „Hybridraketenantriebe“, Wilhelm Goldmann Verlag GmbH, München, 1972
[2] M. J. Chiaverini, K. K. Kuo, „Fundamentals of Hybrid Rocket Combustion and Propulsion“, Progress in Astronautics and Aeronautics Volume 218, 2007
[3] G. Sutton, “Rocket Propulsion Elements”, Wiley-Interscience, 1992, p.582
[4] R. W. Humble, G. N. Henry, W. J. Larson, “Space Propulsion Analysis and Design”, McGraw-Hill Companies Inc., 1995
[5] M. A. Karabeyoglu, D. Altman, B. J. Cantwell, „Combustion of Liquefying Hybrid Propellants: Part 1, General Theory”, Journal of Propulsion and Power, Vol. 18, No. 3, May-June 2002
[6] M. A. Karabeyoglu, B. J. Cantwell, „Combustion of Liquefying Hybrid Propellants: Part 2, Stability of Liquid Films”, Journal of Propulsion and Power, Vol. 18, No. 3, May-June 2002
[7] M. A. Karabeyoglu, G. Zilliac, B. J. Cantwell, S. De Zilwa, P. Castelluci, „Scale-Up Tests of High Regression Rate Liquefying Hybrid Rocket Fuels“ ,41. Aerospace Sciences Meeting and Exhibit, Reno, Nevada, January 2003
[8] G. Zilliac, M. A. Karabeyoglu, „Modeling of Propellant Tank Pressurization“, 41. Joint Propulsion Conference, Tucson, July 2005
[9] L. Casalino, D. Pastrone, “Optimal Design of Hybrid Rockets with Self-Pressurizing Oxidizer”, 42. Joint Propulsion Conference, Sacramento, July 2006
[10] K. Lohner, J. Dyer, E. Doran, Z. Dunn, G. Zilliac, „Fuel Regression Rate Characterization Using a Laboratory Scale Nitrous Oxide Hybrid Propulsion System” , 42. Joint Propulsion Conference, Sacramento, July 2006
[11] M. A. Karabeyoglu, G. Zilliac, P. Castelluci, P. Urbanczyk, J. Stevens, G. Inalhan, B. J. Cantwell „Development of High Burning-Rate Hybrid-Rocket-Fuel Flight Demonstrators“, 39. Joint Propulsion Conference, Huntsville, July 2003

NOMENCLATURE

Abbreviations

a	fuel dependent constant
A	Surface, Area
ATV	Automated Transfer Vehicle
c_d	Discharge coefficient
c_{dn}	Discharge coefficient of nozzle
CEA	Chemical Equilibrium with Applications
CFRP	Carbon Fibre Reinforced Plastic
DLR	Deutsches Zentrum für Luft- und Raumfahrt
G	Mass flux
g	Gravitational acceleration
HTPB	Hydroxyl Terminated PolyButadiene
H_2O_2	Hydrogen peroxide
ISS	International Space Station
L	Fuel grain length
L/D	Length to diameter ratio
LEX	Lithergol experimental series
LOX	Liquid oxygen
NASA	National Aeronautics and Space Administration
N_2O	Nitrous oxide
N_2O_4	Nitrogen tetroxide
O/F	Oxidizer-to-fuel ratio
ONERA	Office Natioal d’Études et de Recherches Aérospatiales
p	Pressure
PBAN	PolyButadiene AcryloNitrile
PE	PolyEthylene
PMMA	PolyMethylMethAcrylate (Plexiglas ®)
PP	PolyPropylene
PVC	PolyVinyl Chloride
TIC	Truncated Ideal Contour
TOC	Thrust Optimized Contour
TOP	Thrust Optimized Parabola
RFNA	Red Fuming Nitric Acid
t	Time
t_b	Burn time
UTC	United Technology Center
$\dot{m}$	Mass flow
$\dot{r}$	Regression rate
ρ	Density

Subscripts or superscripts

c	chamber
f	Fuel
inj	Injector
L	Liquid
m	Length exponent
n	Regression rate exponent
Ox	Oxidizer
p	Port
s	Surface
t	Nozzle throat
tg	Tank gas
α	Pressure exponent